2.4 angstrom crystal structure of an oxaliplatin 1,2-d(GpG) intrastrand cross-link in a DNA dodecamer duplex

Spingler, Bernhard ; Whittington, D A ; Lippard, S J

DOI: https://doi.org/10.1021/ic010790t

Other titles: 2.4 Å Crystal Structure of an Oxaliplatin 1,2-d(GpG) Intrastrand Cross-Link in a DNA Dodecamer Duplex

2.4 Å Crystal Structure of an Oxaliplatin 1,2-d(GpG) Intrastrand Cross-Link in a DNA Dodecamer Duplex

Bernhard Spingler, Douglas A. Whittington, and Stephen J. Lippard*

Department of Chemistry, Massachusetts Institute of Technology, Cambridge, Massachusetts 02139

Received July 25, 2001

(1*R*,2*R*-Diaminocyclohexane)oxalatoplatinum(II) (oxaliplatin) is a third-generation platinum anticancer compound that produces the same type of inter- and intrastrand DNA cross-links as cisplatin. In combination with 5-fluorouracil, oxaliplatin has been recently approved in Europe, Asia, and Latin America for the treatment of metastatic colorectal cancer. We present here the crystal structure of an oxaliplatin adduct of a DNA dodecanucleotide duplex having the same sequence as that previously reported for cisplatin (Takahara, P. M.; Rosenzweig, A. C.; Frederick, C. A.; Lippard, S. J. *Nature* **1995**, *377*, 649−652). Pt-MAD data were used to solve this first X-ray structure of a platinated DNA duplex derived from an active platinum anticancer drug other than cisplatin. The overall geometry and crystal packing of the complex, refined to 2.4 Å resolution, are similar to those of the cisplatin structure, despite the fact that the two molecules crystallize in different space groups. The platinum atom of the {Pt(*R*,*R*-DACH)}$^{2+}$ moiety forms a 1,2-intrastrand cross-link between two adjacent guanosine residues in the sequence 5′-d(CCTCTGGTCTCC), bending the double helix by ∼30° toward the major groove. Both end-to-end and end-to-groove packing interactions occur in the crystal lattice. The latter is positioned in the minor groove opposite the platinum cross-link. A novel feature of the present structure is the presence of a hydrogen bond between the pseudoequatorial NH hydrogen atom of the (*R*,*R*)-DACH ligand and the O6 atom of the 3′-G of the platinated d(GpG) lesion. This finding provides structural evidence for the importance of chirality in mediating the interaction between oxaliplatin and duplex DNA, calibrating previously published models used to explain the reactivity of enantiomerically pure vicinal diamine platinum complexes with DNA in solution. It also provides a new kind of chiral recognition between an enantiomerically pure metal complex and the DNA double helix.

Introduction

cis-Diamminedichloroplatinum(II) **1** (cisplatin, Figure 1) received FDA approval in 1979 for use as an anticancer drug. Cisplatin is widely used and is especially effective against testicular, head, neck, non-small-cell lung, and cervical cancers.[1] DNA is generally agreed to be the biological target of cisplatin,[2,3] with the major adduct being a 1,2-intrastrand cross-link between the N7 atoms of two adjacent purine residues, either d(GpG) or, less frequently, d(ApG).[4] X-ray structures of cisplatin bound to several different DNA sequences have been reported, providing insight into the structural changes that occur upon platination. Initially, several short, single-stranded deoxynucleosides containing the *cis*-[Pt(NH$_3$)$_2$\{d(pGpG)\}] unit were examined. These structures exhibited large dihedral angles of 76−87° between the two cisplatin-modified guanine bases.[5−7] The first single-crystal X-ray structure of double-stranded DNA harboring a well-defined cisplatin adduct was reported in 1995.[8,9]

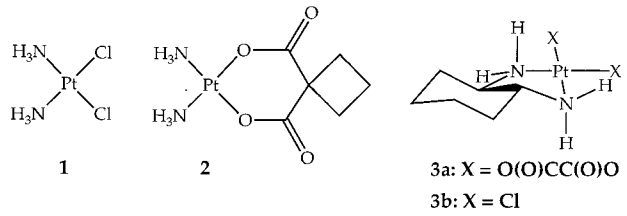

Figure 1. Structures of cisplatin (**1**), carboplatin (**2**), and (1*R*,2*R*)-diaminocyclohexaneplatinum(II) (**3**) complexes including oxaliplatin (**3a**).

Cisplatin coordination forces the duplex to bend significantly toward the major groove without disrupting Watson−Crick base pairing. Hydrogen bonding occurs between the oxygen atom of the 5′ phosphate group and an NH$_3$ ligand on platinum. The main portion of the duplex, starting from the 5′ end, adopts the A-DNA conformation, and there is a switch to B-form DNA of the 3′ end. A recent analysis of the cisplatin 12-mer crystal structure with the program 3DNA, using the z_P parameter to delineate A- from B-DNA, reveals the A/B junction to be distributed over two base pair steps.[10] The same cisplatin-modified 12-mer was studied in solution by NMR spectroscopy,[11] allowing comparisons to be made between the solid and

* Author to whom correspondence should be addressed. E-mail: lippard@lippard.mit.edu.

(1) Sherman, S. E.; Lippard, S. J. *Chem. Rev.* **1987**, *87*, 1153−1181.
(2) Jamieson, E. R.; Lippard, S. J. *Chem. Rev.* **1999**, *99*, 2467−2498.
(3) Lippert, B. *Cisplatin: Chemistry and Biochemistry of a Leading Anticancer Drug*; John Wiley & Sons Ltd.: New York, 1999.
(4) Eastman, A. *Pharmacol. Ther.* **1987**, *34*, 155−166.
(5) Sherman, S. E.; Gibson, D.; Wang, A. H.-J.; Lippard, S. J. *Science* **1985**, *230*, 412−417.
(6) Sherman, S. E.; Gibson, D.; Wang, A. H.-J.; Lippard, S. J. *J. Am. Chem. Soc.* **1988**, *110*, 7368−7381.
(7) Admiraal, G.; van der Veer, J. L.; de Graaff, R. A. G.; den Hartog, J. H. J.; Reedijk, J. *J. Am. Chem. Soc.* **1987**, *109*, 592−594.
(8) Takahara, P. M.; Rosenzweig, A. C.; Frederick, C. A.; Lippard, S. J. *Nature* **1995**, *377*, 649−652.
(9) Takahara, P. M.; Frederick, C. A.; Lippard, S. J. *J. Am. Chem. Soc.* **1996**, *118*, 12309−12321.
(10) Lu, X.-J.; Shakked, Z.; Olson, W. K. *J. Mol. Biol.* **2000**, *300*, 819−840.

10.1021/ic010790t CCC: $20.00
Published on Web 09/19/2001

solution structures. In the solution structure, the DNA duplex is considerably more bent, and the dihedral angle between the planes of the cross-linked guanine bases is also much larger. A second NMR structure containing a platinum complex having the *N*-oxide spin label ligand 4-amino-TEMPO, bound similarly to a DNA undecamer,[12] shows a conformational change of DNA neighboring the platinum coordination site from A-like to B-like DNA.

The cytotoxicity of cisplatin most likely involves the interaction of certain cellular proteins with the cisplatin-modified DNA.[13] The first X-ray crystal structure of a cisplatin-modified 16-mer duplex complexed with one such protein, domain A of the high mobility group (HMG) protein HMG-1, revealed that the protein interacts mainly with the minor groove of the DNA, which is widened and bent toward the major groove.[14] A novel feature of this protein−DNA complex is the intercalation of a phenylalanine between the two cross-linked guanosine residues. Interestingly, the coordination geometry at platinum better resembles that in the cisplatin-modified single-strand dinucleotide d(pGpG) structures[6,14] than the geometries observed in the solution structures or the 12-mer X-ray crystal structure. Recent NMR studies of a cisplatin-modified DNA 9-mer concluded that the choice of DNA starting model used in NMR-restrained molecular dynamics refinements was crucial in determining the geometry of the final minimized structure.[15] Only when the conformation of the sugar−phosphate backbone from the platinated 16-mer/HMG1 domain A crystal structure was used did the NMR data refine to a satisfactory result. On the basis of these results, the authors predicted that all 1,2-intrastrand platinum-modified duplexes containing a d(XG*G*) or d(XA*G*) sequence (X = C or T) would have a similar structure in solution, with the XN (N = A* or G*) base pair step having a large positive shift and slide.

Although cisplatin (**1**) is a very effective anticancer drug, it has many undesirable side effects, and inherent and acquired resistance reduces its clinical efficacy. A number of less toxic second-generation compounds have been synthesized, most notably carboplatin **2** (Figure 1).[16] (1*R*,2*R*-Diaminocyclohexane)oxalatoplatinum(II) **3a** (oxaliplatin, Figure 1) is a third-generation platinum compound[17] that produces the same kind of inter- and intrastrand DNA cross-links as cisplatin.[18] Oxaliplatin, in combination with 5-fluorouracil, has been recently approved in Europe, Asia, and Latin America[19] but not in the U.S.A.,[20] for the treatment of metastatic colorectal cancer.

The stereochemistry of the 1,2-diaminocyclohexane moiety significantly influences the toxicity of the platinum complexes toward various cancer cell lines. Complexes of the two trans diastereomers (*R*,*R* and *S*,*S*) exhibit higher activities than the meso (*R*,*S* and *S*,*R*) adducts, and the *R*,*R* complex is more effective than the *S*,*S*.[21−24] Although oxaliplatin forms fewer lesions than cisplatin, it is more cytotoxic against some cell lines.[25] During replication, translesion synthesis catalyzed by DNA polymerases (pol) β, ζ, γ, and η is more efficient, but also more error prone, past oxaliplatin adducts than past cisplatin adducts.[26,27] From a study of the kinetics of nucleotide insertion opposite Pt−GG adducts by mammalian pol β, it was predicted that "the oxaliplatin and cisplatin−GG adducts will show the greatest conformational differences in the vicinity of the 3′-G(Pt)".[28] Furthermore, both HMG1[26] and its isolated HMG domains A and B demonstrate lower affinity for oxaliplatin−DNA adducts than the corresponding cisplatin lesions.[29]

Little structural information exists for oxaliplatin DNA adducts. The complexes of ((1*R*,2*R*)-diaminocyclohexane)platinum(II), (*R*,*R*)-DACH−Pt(II), with either two deoxyguanosine 5′-monophosphates[30] or d(GpG)[31] have been investigated by ^{1}H NMR spectroscopy. Molecular modeling studies of cisplatin or (*R*,*R*)-DACH−Pt(II) bound to a duplex dodecamer propose a geometry around the platinum atom of the oxaliplatin cross-link similar to that in the corresponding cisplatin structures.[32] Only in the cisplatin model, however, was a hydrogen bond predicted to form between the 3′ amine and the carbonyl oxygen (O6) of the guanosine. It has been proposed that the hydrophobic cyclohexane ring changes the overall DNA geometry, but there is no experimental confirmation of this hypothesis.

Studies of (2*R*,3*R*)- and (2*S*,3*S*)-diaminobutane(DAB)platinum(II) complexes bound to natural DNA and synthetic oligodeoxyribonucleotide duplexes in a cell-free medium revealed the influence of the stereogenic centers of the ligand upon the overall geometry. Reaction of these DNA-damaging agents indicated the DNA to be more distorted on the 3′/5′ sides of the cross-link for the (*R*,*R*)-/(*S*,*S*)-DAB−Pt complexes, respectively.[33] These results support the notion that a hydrogen bond forms in solution between an amino group and the O6 atom of a coordinated guanine cis to that group. Such an interaction was observed in small molecule crystal structures containing the {PtN_2(Gua)} moiety, where N is an achiral (di)amine and Gua a 6-oxo purine,[34−37] as well in a molecular modeling study of a single-stranded platinated DNA.[38]

Only duplex oligonucleotides containing cisplatin adducts have thus far been investigated by single-crystal X-ray analysis.

(11) Gelasco, A.; Lippard, S. J. *Biochemistry* **1998**, *37*, 9230−9239.
(12) Dunham, S. U.; Dunham, S. U.; Turner, C. J.; Lippard, S. J. *J. Am. Chem. Soc.* **1998**, *120*, 5395−5406.
(13) Zlatanova, J.; Yaneva, J.; Leuba, S. H. *FASEB J.* **1998**, *12*, 791−799.
(14) Ohndorf, U.-M.; Rould, M. A.; He, Q.; Pabo, C. O.; Lippard, S. J. *Nature* **1999**, *399*, 708−712.
(15) Marzilli, L. G.; Saad, J. S.; Kuklenyik, Z.; Keating, K. A.; Xu, Y. *J. Am. Chem. Soc.* **2001**, *123*, 2764−2770.
(16) Reedijk, J. *Chem. Commun.* **1996**, 801−806.
(17) Kidani, Y.; Inagaki, K.; Saito, R.; Tsukagoshi, S. *J. Clin. Hematol. Oncol.* **1977**, *7*, 197−209.
(18) Boudny, V.; Vrana, O.; Gaucheron, F.; Kleinwachter, V.; Leng, M.; Brabec, V. *Nucleic Acids Res.* **1992**, *20*, 267−272.
(19) Graham, M. A.; Lockwood, G. F.; Greenslade, D.; Brienza, S.; Bayssas, M.; Gamelin, E. *Clin. Cancer Res.* **2000**, *6*, 1205−1218.
(20) *Ann. Oncol.* **2000**, *11*, 640.
(21) Kidani, Y.; Inagaki, K.; Iigo, M.; Hoshi, A.; Kuretani, K. *J. Med. Chem.* **1978**, *21*, 1315−1318.
(22) Kidani, Y.; Noji, M.; Tashiro, T. *Gann* **1980**, *71*, 637−643.
(23) Noji, M.; Okamoto, K.; Kidani, Y.; Tashiro, T. *J. Med. Chem.* **1981**, *24*, 508−515.
(24) Hambley, T. W. *Coord. Chem. Rev.* **1997**, *166*, 181−223.
(25) Woynarowski, J. M.; Chapman, W. G.; Napier, C.; Herzig, M. C. S.; Juniewicz, P. *Mol. Pharmacol.* **1998**, *54*, 770−777.
(26) Vaisman, A.; Lim, S. E.; Patrick, S. M.; Copeland, W. C.; Hinkle, D. C.; Turchi, J. J.; Chaney, S. G. *Biochemistry* **1999**, *38*, 11026−11039.
(27) Vaisman, A.; Masutani, C.; Hanaoka, F.; Chaney, S. G. *Biochemistry* **2000**, *39*, 4575−4580.
(28) Vaisman, A.; Chaney, S. G. *J. Biol. Chem.* **2000**, *275*, 13017−13025.
(29) Wei, M.; Cohen, S. M.; Silverman, A. P.; Lippard, S. J. *J. Biol. Chem.* **2001**, in press.
(30) Pasini, A.; De Giacomo, L. *Inorg. Chim. Acta* **1996**, *248*, 225−230.
(31) Inagaki, K.; Nakahara, H.; Alink, M.; Kidani, Y. *Inorg. Chem.* **1990**, *29*, 4496−4500.
(32) Scheeff, E. D.; Briggs, J. M.; Howell, S. B. *Mol. Pharmacol.* **1999**, *56*, 633−643.
(33) Malina, J.; Hofr, C.; Maresca, L.; Natile, G.; Brabec, V. *Biophys. J.* **2000**, *78*, 2008−2021.
(34) Lippert, B.; Raudaschl, G.; Lock, C. J. L.; Pilon, P. *Inorg. Chim. Acta* **1984**, *93*, 43−50.
(35) Heyl, B. L.; Shinozuka, K.; Miller, S. K.; VanDerveer, D. G.; Marzilli, L. G. *Inorg. Chem.* **1985**, *24*, 661−666.
(36) Sindellari, L.; Schöllhorn, H.; Thewalt, U.; Raudaschl-Sieber, G.; Lippert, B. *Inorg. Chim. Acta* **1990**, *168*, 27−32.
(37) Grabner, S.; Plavec, J.; Bukovec, N.; Di Leo, D.; Cini, R.; Natile, G. *J. Chem. Soc., Dalton Trans.* **1998**, 1447−1451.
(38) Kozelka, J.; Fouchet, M.-H.; Chottard, J.-C. *Eur. J. Biochem.* **1992**, *205*, 895−906.

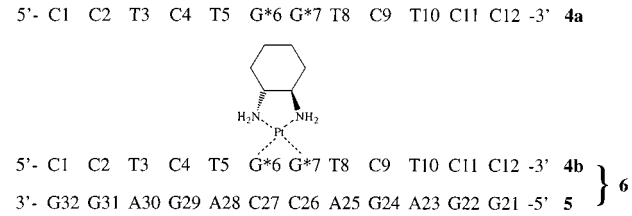

Figure 2. Oligonucleotide sequences used in this work.

Furthermore, there exists no experimental structure of a lesion formed by oxaliplatin coordinated to double-stranded DNA. We report here the synthesis and crystallization of a 12-mer duplex DNA containing a 1,2-d(GpG) oxaliplatin intrastrand cross-link (**6**) in a sequence identical to that investigated previously for cisplatin-modified DNA structures (Figure 2).[8,9,11] The structure affords deeper insights into the differences between cisplatin and oxaliplatin, a molecular level view of the different interactions of the enantiomers of *trans*-vicinal diamino ligands with DNA, and some commonality of the overall structures of platinated DNA lesions determined previously. These findings should aid further the design of better platinum antitumor drugs.

Experimental Section

Materials. (1*R*,2*R*)-Diaminocyclohexane was obtained from Aldrich, and potassium tetrachloroplatinate(II), K_2PtCl_4, was provided by Johnson-Matthey. Phosphoramidites and reagents for DNA synthesis were purchased from Glen Research. Crystallization reagents were obtained from Aldrich, Fluka, Mallinckrodt, and Sigma.

High-pressure liquid chromatography (HPLC) was carried out on a Waters 600E system controller with a Waters 486 detector ($\lambda = 260$ nm) for preparative runs or on a Waters 600S controller and Waters 2487 detector ($\lambda = 260$ nm) for analytical runs. Atomic absorption spectroscopy was performed using a Varian AA1475 instrument.

Synthesis and Characterization of (1*R*,2*R*)-Diaminocyclohexanedichloroplatinum(II) (3b). (1*R*,2*R*)-Diaminocyclohexanedichloroplatinum(II) (**3b**) was prepared from (1*R*,2*R*)-diaminocyclohexane and potassium tetrachloroplatinate(II) in 82% yield as described.[21] It was fully characterized by ^{1}H, ^{13}C, and ^{195}Pt NMR spectroscopy (see Supporting Information). Slow evaporation from DMF yielded colorless crystals of **3b**·DMF after 1 month, which were suitable for X-ray analysis. The crystal structure determination was carried out on a Bruker (formerly Siemens) CCD diffractometer with graphite-monochromatized Mo Kα radiation ($\lambda = 0.71073$ Å) controlled by a Pentium-based PC running the SMART software package.[39] Single crystals were mounted at room temperature on the ends of glass fibers in Paratone N oil, and data were collected for 20 s per frame at 188 K in a stream of cold dinitrogen maintained by a Bruker LT-2A nitrogen cryostat. Data collection and reduction protocols are described in detail elsewhere.[40] The structure was solved by direct methods and refined using the SHELXL97 software package.[41] Hydrogen atoms were assigned idealized locations. Empirical absorption corrections were applied by using SADABS.[42] Relevant crystallographic information is given in Figure S1 and Tables S1−S4 (Supporting Information).

Deoxyoligonucleotide Synthesis and Purification. Figure 2 shows three single-stranded DNAs that were prepared according to procedures reported previously.[9] The deoxyoligonucleotides were synthesized on a 10 μmol scale with an Applied Biosystems 392 DNA/RNA automated synthesizer by using conventional phosphoramidite solid support methodology.[43] Protecting groups were removed by G25 Sephadex size exclusion chromatography. The top strand, to be platinated, was passed through an ion exchange DOWEX column in order to replace the ammonium by sodium ions, since the former might react with platinum in a subsequent step.

A 21 mM aqueous solution of (1*R*,2*R*)-diaminocyclohexane platinum(II) dichloride (**3b**) was activated by treatment with 1.98 equiv of silver nitrate and agitation overnight in the dark. The suspension was centrifuged and the mother liquor transferred to another vial and centrifuged again. A 1.1 equiv portion of the solution containing the activated (*R*,*R*)-DACH−Pt(II) was added to 10 mL of a 0.414 mM (4.14 μmol) aqueous solution of **4a**. The reaction, carried out in the dark at 37 °C, was complete in 90 min, as revealed by analytical ion exchange HPLC, and was terminated by freezing. The platinated product **4b** and the complementary bottom strand **5** were purified on a preparative ion exchange HPLC column, eluting with a 150−300 mM linear NaCl gradient and subsequently with a 5−20% acetonitrile gradient on a preparative reverse phase C4 HPLC column.

A 0.998 mL aliquot of a 1.053 mM solution of the top strand **4b** (1.05 μmol) and 0.263 mL of a 4.00 mM solution of the bottom strand **5** (1.05 μmol) were annealed by mixing for 10 min at room temperature. The annealed double strand **6** was purified by a 0.2 M to 0.5 M lithium chloride gradient on a preparative ion exchange HPLC column to give 0.645 μmol of **6** with an r_b ratio of 0.986. A solution of **6** was divided into equal aliquots, each containing 240 μg of DNA. The aliquots were heated to 80 °C, allowed to cool to room temperature within 6 h, then cooled to 4 °C for 1 h, and finally lyophilized and stored at −20 °C.

Crystallization of 6. The hanging drop vapor diffusion method was used for crystallization,[44] starting with conditions from two different sparse matrix crystallization screens.[45,46] Crystals were grown at 4 °C from 3.0 μL drops containing 0.2 mM DNA, 2.5% or 5% MPD ((±)-2-methyl-2,4-pentanediol), 20 mM sodium cacodylate (pH 7.0), 6 mM spermine·4HCl, 10 mM barium chloride, and 2.5% ethyl acetate equilibrated against a reservoir of 20% or 30% MPD and 5% ethyl acetate. Crystals with maximum dimensions of 0.08 × 0.2 × 0.4 mm^3 appeared after 5 days.

X-ray Data Collection of 6. Crystals were transferred to a solution of 30% MPD, 40 mM sodium cacodylate (pH 7.0), 12 mM spermine·4HCl, 20 mM barium dichloride, and 5% ethyl acetate at 4 °C, then mounted in loops, and flash frozen. Multiwavelength anomalous diffraction (MAD) studies[47] using **6** were conducted at 100 K on beamline 19-ID of the Structural Biology Center-CAT at the Advanced Photon Source at Argonne National Laboratory. The platinum absorption spectrum was measured as X-ray fluorescence using a Bicron scintillation counter. The values of f' and f'' were calculated with the program CHOOCH.[48] Four wavelengths were selected for data collection corresponding to the inflection point (1.0724 Å), the peak (1.0721 Å), and two remote energies (1.0277, 1.1206 Å) with respect to the absorption edge of platinum. Complete data sets were collected successively for each wavelength on the SBC APS1 3 × 3 CCD detector. Each data set required approximately 12 min to collect (100 frames, 1° each, 4 s/frame). Intensities were integrated using DENZO and scaled with SCALEPACK.[49]

Subsequently, data from a crystal of **6** grown under lower MPD concentrations were collected at beamline 9-1 of the Stanford Synchrotron Radiation Laboratory (wavelength 0.970 Å, Mar Research imaging plate detector, 100 frames, 2° each, 32 s/frame) to 2.4 Å resolution and processed with the HKL suite of programs.[49] Data collection statistics are summarized in Table 1.

Structure Determination and Refinement of 6. MAD phases were calculated by using the program CNS (v 1.0) for the space groups *I*222 and $I2_12_12_1$.[50] After solvent flattening, only the phase information for

(39) *SMART*, 5.05 ed.; Bruker AXS, Inc.: Madison, WI, 1998.
(40) Feig, A. L.; Bautista, M. T.; Lippard, S. J. *Inorg. Chem.* **1996**, *35*, 6892−6898.
(41) Sheldrick, G. M. *SHELXL97-2: Program for the Refinement of Crystal Structures*; University of Göttingen: Göttingen, 1997.
(42) Sheldrick, G. M. *SADABS: Area-Detector Absorption Correction*; University of Göttingen: Göttingen, 1996.
(43) Gait, M. J. *Oligonucleotide Synthesis: A practical approach*; IRL Press Ltd.: Oxford, 1984.
(44) Drenth, J. *Principles of Protein X-ray Crystallography*; Springer: New York, 1994.
(45) Scott, W. G.; Finch, J. T.; Grenfell, R.; Fogg, J.; Smith, T.; Gait, M. J.; Klug, A. *J. Mol. Biol.* **1995**, *250*, 327−332.
(46) Berger, I.; Kang, C.; Sinha, N.; Wolters, M.; Rich, A. *Acta Crystallogr.* **1996**, *D52*, 465−468.
(47) Walsh, M. A.; Evans, G.; Sanishvili, R.; Dementieva, I.; Joachimiak, A. *Acta Crystallogr.* **1999**, *D55*, 1726−1732.
(48) Evans, G.; Pettifer, R. F. *J. Appl. Crystallogr.* **2001**, *34*, 82−86.
(49) Otwinowski, Z.; Minor, W. *Methods Enzymol.* **1997**, *276*, 307−326.

Table 1. Data Collection and Refinement Statistics for **6**

Data Collection

	$\lambda 1^a$	$\lambda 2^a$	$\lambda 3^a$	$\lambda 4^a$	high resolution[b]
wavelength (Å)	1.0721	1.0724	1.0277	1.1206	0.970
a (Å)	42.492	42.500	42.490	42.501	41.942
b (Å)	49.468	49.462	49.503	49.480	51.246
c (Å)	85.639	85.614	85.491	85.605	87.049
resolution range (Å)	25−2.8	25−2.8	25−2.8	25−2.8	100−2.4
obsd reflns	34018	34232	34101	33882	61465
unique reflns	2371	2369	2369	2365	6296
completeness[c] (%)	96.1 (76.4)	96.4 (80.8)	95.7 (73.4)	95.5 (72.0)	93.7 (69.0)
R_{sym}[c,d] (%)	10.5 (42.9)	8.5 (46.1)	7.6 (46.4)	6.2 (51.5)	8.9 (36.8)
$\langle I/\sigma \rangle$[c]	19.1 (3.2)	35.6 (3.2)	35.6 (3.3)	35.3 (2.6)	18.9 (4.5)
phasing power[e]	4.0	3.7	2.6	1.7	

Refinement

	high resolution[b]
R[f] [4448 reflns with $F_o > 4\sigma(F_o)$]	0.209
R_{free}[g] [487 reflns with $F_o > 4\sigma(F_o)$]	0.256
rmsd bond lengths (Å)	0.007
rmsd 1,3 distances (angles) (Å)	0.021
rmsd planes (for 252 atoms) (Å)	0.0005
no. of refined params	2052
no. of restraints	2360

[a] Crystals grown from 5% MPD solutions, measured at the SBC-19ID beamline at the Advanced Photon Source. [b] Crystals grown from 2.5% MPD solutions, measured at the beamline 9-1 at the Stanford Synchrotron Radiation Laboratory. [c] Values in parentheses for the highest resolution shell. [d] $R_{sym} = \sum|I - \langle I \rangle|/\sum I$. [e] Phasing power = $[(\sum F_h^2)/(\text{rms lack of closure})]^{0.5}$. [f] $R = \sum||F_o| - |F_c||/\sum|F_o|$. [g] $R_{free} = R$ obtained for a test set of reflections (10% of the diffraction data).

Figure 3. Solvent flattened initial electron density map of **6** using the 2.8 Å resolution data and showing the end-to-end intermolecular DNA stacking. Green color depicts the 1σ contour level and purple, the 5σ level.

*I*222 produced a readily interpretable electron density map (Figure 3). An initial model was then subjected to rigid body refinement.[50] Data to 2.8 Å resolution were used for cycles of positional, simulated-annealing, and *B*-factor refinements, interspersed with analysis of the geometry of the model. A peak of high electron density found at a distance of 2.6 Å to N7 of G31 was modeled as a fully occupied barium ion. 10% of the initial reflections were set aside for use in calculating R_{free}.[51−53] Manual model rebuilding was performed in O.[54] Phases from a model with $R_{free} = 32.7\%$ and $R = 29.5\%$ were applied for a similar series of refinement cycles using the 2.4 Å data set. Refinements were completed by using a slightly modified program version of SHELXL97[41] in which the HOPE parameter[55] was set to neutral if it became negative for some reflections during the refinement. The DNA Dictionary for SHELXL was used with the appropriate restraints for the phosphodiester backbone, sugars, and nucleobases.[56,57] The DACH ligand, bound to platinum, was refined with 1,2- and 1,3-distance restraints. Twelve water molecules were added at locations having proper distance for hydrogen-bonding interactions and electron densities greater than 1.0σ on a $|2|F_o| - |F_c||$ map and 2.0σ on an $||F_o| - |F_c||$ map. Except for the barium cation, no other counterions were found to be associated with the DNA backbone. Refinement statistics are given in Table 1. The geometry parameters were calculated with the programs 3DNA,[10] Curves,[58] Freehelix,[59] MacMoMo,[60] MadBend,[61] and PLATON.[62] The atomic coordinates for the final, refined model have been deposited in the Nucleic Acid Database with accession number DD0040 (PDB file number: 1IHH).

Results

X-ray Structure of 3b. The structure of (1*R*,2*R*)-diaminocyclohexanedichloroplatinum(II) (**3b**) is depicted in Figure 4. Crystallographic data for (**3b**·DMF) are given in Table S1. The

(50) Brünger, A. T.; Adams, P. D.; Clore, G. M.; DeLano, W. L.; Gros, P.; Grosse-Kunstleve, R. W.; Jiang, J.-S.; Kuszewski, J.; Nilges, M.; Pannu, N. S.; Read, R. J.; Rice, L. M.; Simonson, T.; Warren, G. L. *Acta Crystallogr.* **1998**, *D54*, 905−921.

(51) Brünger, A. T. *Nature* **1992**, *355*, 472−474.
(52) Brünger, A. T. *Acta Crystallogr.* **1993**, *D49*, 24−36.
(53) Kleywegt, G. J.; Brünger, A. T. *Structure* **1996**, *4*, 897−904.
(54) Jones, T. A.; Zou, J.-Y.; Cowan, S. W.; Kjeldgaard, M. *Acta Crystallogr.* **1991**, *A47*, 110−119.
(55) Parkin, S.; Moezzi, B.; Hope, H. *J. Appl. Crystallogr.* **1995**, *28*, 53−56.
(56) Clowney, L.; Jain, S. C.; Srinivasan, A. R.; Westbrook, J.; Olson, W. K.; Berman, H. M. *J. Am. Chem. Soc.* **1996**, *118*, 509−518.
(57) Gelbin, A.; Schneider, B.; Clowney, L.; Hsieh, S.-H.; Olson, W. K.; Berman, H. M. *J. Am. Chem. Soc.* **1996**, *118*, 519−529.
(58) Lavery, R.; Sklenar, H. *J. Biomol. Struct. Dyn.* **1988**, *6*, 63−91.
(59) Dickerson, R. E. *J. Mol. Biol.* **1998**, *26*, 1906−1926.
(60) Dobler, M. *MacMoMo*; Zürich, Switzerland, 1995.
(61) Strahs, D.; Schlick, T. *J. Mol. Biol.* **2000**, *301*, 643−663.
(62) Spek, A. L. *PLATON—A Multipurpose Crystallographic Tool*; Utrecht University: Utrecht, 2000.

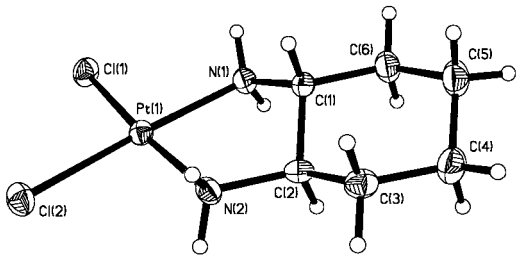

Figure 4. ORTEP plot of (1*R*,2*R*)-diaminocyclohexanedichloroplatinum(II) (**3b**) showing 50% probability thermal ellipsoids.

two molecules in the asymmetric unit have almost identical geometry. The platinum atoms are distorted square planar with adjacent angles between 83.6(2)° and 94.88(7)°. The cyclohexane rings have a typical chair conformation.

Unit Cell Composition and Crystal Packing of 6. The asymmetric unit contains one molecule of **6**. The crystals have a Matthew's coefficient of 2.82, corresponding to a solvent content of about 55%. There are two types of interactions between the duplexes in the lattice: end-to-end, produced by the dyad perpendicular to the DNA axis, Figures 3 and S4 (Supporting Information), and end-to-minor groove. Both interactions, mediated by several hydrogen bonds (see below), were also present in the structure of the cisplatin analogue.[8,9] The end-to-end contact, typical for B-DNA,[63] places the 3′ C12 base of one duplex stacked on the 5′ G21 of another, thereby forming a pseudohelix. In the end-to-minor groove interaction, the 5′ terminal base pair, C1−G32, packs against the minor groove opposite the platinum binding site of a neighboring duplex. Such a packing motif is often seen in A-DNA[64] and is present in the cisplatin−DNA structure. In this interaction, the O3′ hydroxyl of G32 donates its hydrogen to O2 of T8 and O2 of C26. Twelve water molecules were located, forming hydrogen bonds to the DNA (see Figure S2, Supporting Information).

The Platinated DNA Duplex. The two strands maintain their hydrogen bond base pairing throughout the entire helix despite the coordination of platinum. The base pair parameters and sugar conformations are shown in Figure 5 and Table 2, respectively. Additional base pair step parameters appear in Tables S5−S8 and Figure S3 in the Supporting Information. The first seven base pair steps including C1−G32 through T8−A25 adopt an A-DNA-like conformation, and the two last steps, T10−A23 through C12−G21, are very similar to B-DNA, judging by the slide, z_p, sugar puckering, and minor/major groove parameters. In accord with a recent analysis of A-form motifs in ligand-bound DNA structures,[10] we also find that the A/B junction is distributed over two dimer steps, between the base pairs T8−A25 and T10−A23. As seen in the previous structural determination of cisplatin-modified DNA, the minor groove is widened whereas the major groove has become even narrower than the minor groove (Table S9, Supporting Information). The two planes of the nucleobases G6 and G7 form a dihedral angle of 25°. The pseudoequatorial hydrogen of the NH_2 group of the DACH ligand cis to the N7 atom of guanine G7 forms a hydrogen bond to oxygen O6 of G7 (N−O distance, 2.9 Å; angle of N−H···O, 136°; Figure 6). In the cisplatin analogue, the corresponding N−O distance is 3.5 Å. The shortest distance between the other DACH amino nitrogen atom, cis to N7 of G6, and the oxygen atom of the next phosphate group in the 5′

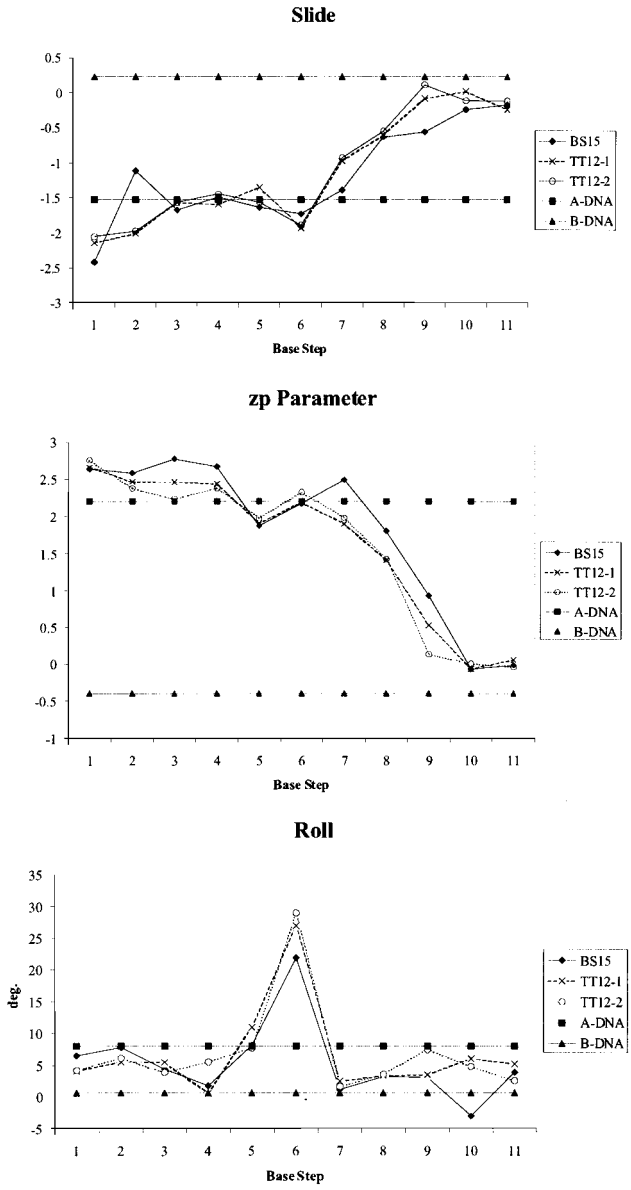

Figure 5. Roll, slide, and z_p parameters for **6**, TT12-1, and TT12-2;[8,9] calculated with the program 3DNA.[10]

direction is 4.6 Å. The distance of this atom to O6 of G6 is 4.4 Å. Both values are too long for hydrogen bond formation. The platinum atom has a strongly distorted square-planar environment, with cis angles between the nitrogen donor atoms ranging from 80° to 98°. The platinum atom is displaced from the mean planes of G6 and G7 by 1.3 and 0.8 Å, respectively.

Bend Angle. The bend angles of DNA structures containing a 1,2-G,G intrastrand platinum cross-link, calculated with MadBend[61] based on the local base pair steps from the various programs, are given in Table 3. Previously, the bend angles of platinum-modified duplex DNA structures have always been calculated by taking the two axes defined by base pairs at the 5′ and 3′ ends of the helix and calculating the angle between the two lines projected onto a common plane. The recently published program MadBend allows one to calculate an overall bend angle by using local base pair step parameters. The calculated bend angles for various published structures of platinated DNA vary greatly, however, depending on the program used to calculate the local base pair step parameters, as revealed by the results in Table 3.

(63) Wang, A. H.-J.; Teng, M.-K. *J. Cryst. Growth* **1988**, *90*, 295−310.
(64) Wahl, M. C.; Sundaralingam, M. In *Oxford Handbook of Nucleic Acid Structure*; Neidle, S., Ed.; Oxford University Press: Oxford, 1998; pp 117−144.

Table 2. Sugar Conformational Parameters for **6**

strand I				strand II			
base	tm[a] (deg)	*P*[b] (deg)	puckering	base	tm[a] (deg)	*P*[b] (deg)	puckering
1 C	40.9	26.0	C3′-endo	21 G	38.7	340.2	C2′-exo
2 C	34.7	25.0	C3′-endo	22 G	41.1	25.7	C3′-endo
3 T	42.8	19.9	C3′-endo	23 A	39.3	19.1	C3′-endo
4 C	41.0	23.3	C3′-endo	24 G	37.8	20.6	C3′-endo
5 T	29.7	19.2	C3′-endo	25 A	50.9	43.1	C4′-exo
6 G	37.2	39.5	C4′-exo	26 C	41.1	24.5	C3′-endo
7 G	38.8	20.4	C3′-endo	27 C	38.5	19.9	C3′-endo
8 T	36.2	32.8	C3′-endo	28 A	37.3	31.4	C3′-endo
9 C	30.5	29.6	C3′-endo	29 G	48.2	146.1	C2′-endo
10 T	22.8	123.5	C1′-exo	30 A	28.9	175.1	C2′-endo
11 C	40.9	132.0	C1′-exo	31 G	49.4	170.9	C2′-endo
12 C	38.0	69.6	C4′-exo	32 G	30.3	224.4	C4′-endo
A-DNA[c]	42	18	C3′-endo	A-DNA[c]	42	18	C3′-endo
B-DNA[d]	46	154	C2′-endo	B-DNA[d]	46	154	C2′-endo

[a] tm: amplitude of pseudorotation of the sugar ring. [b] *P*: phase angle of pseudorotation of the sugar ring. [c] See ref 70. [d] See ref 71.

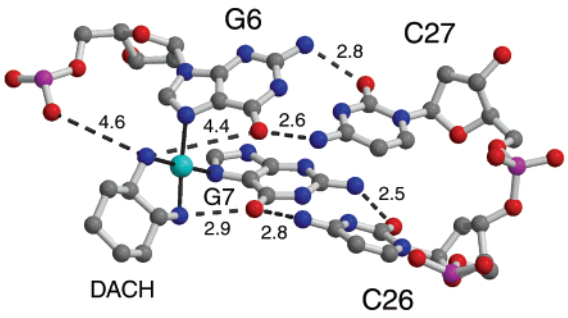

Figure 6. Close-up of **6** showing the GG base pair step together with the bound Pt−DACH complex. The nitrogen atom of the DACH ligand cis to N7 of G7 forms a hydrogen bond to O6 of G7 via the pseudoequatorial hydrogen. Picture drawn with the programs Molscript[72] and Raster3D.[73]

Barium Binding to N7 of G31. Barium is the only other cation located in the structure apart from platinum. It coordinates to N7 and O6 of G31 and forms a bridge to the adjacent purine base A30 by binding to N7 of this residue. A water molecule is the fourth ligand bound to the cation. We assign the geometry as a distorted octahedron, with angles ranging between 66° and 90°. Two missing ligands were not accounted for by the electron density. This example is the first in which a barium cation has been discovered to bridge an adenine and a guanine, although Ba^{2+} links two guanines in an intrastrand manner in A-DNA[65] and in an interstrand fashion in Z-DNA.[66]

Discussion

Structures of [Pt((*R*,*R*)-DACH)Cl_2] and Its DNA Adduct with 6. As indicated in Figure 4, the X-ray structure of [Pt((*R*,*R*)-DACH)Cl_2] reveals a chelate ring in the λ-gauche conformation, a geometry encountered previously in related (*R*,*R*)-DACH−Pt structures.[67,68] Addition of the Ag^+-activated form of **3b** to **4a** readily affords the desired site-specifically platinated dodecanucleotide **4b**, and annealing to **5** leads to the oxaliplatin-modified DNA duplex **6**. This species crystallized in space group *I*222 with one molecule in the asymmetric unit, compared to the cisplatin analogue, which had two molecules per unit cell in space group *P*1. Only one other DNA structure has been reported in space group *I*222.[69]

Despite the different space group and unit cell packing, the overall geometry of **6** is similar to that of the cisplatin analogue with respect to the helix bend angle, mainly A-DNA conformation, and end-to-end and end-to-minor groove intermolecular DNA contacts. The parameters of slide, z_p, and roll (Figure 5), as well as rise, shift, and twist (Figure S3) are graphically displayed together with those for the two molecules of the cisplatin analogue (named TT12-1 and TT12-2) and for canonical A- and B-DNA duplexes. From these plots it is clear that the parameters for the roll, shift, slide, z_p, and, to a lesser extent, rise are all very similar. This similarity is also manifest by the low rmsd values, calculated for all common atoms, of 0.86 Å for **6** and molecule A (TT12-1) of the cisplatin−dodecamer and 0.87 Å for **6** and molecule B (TT12-2). TT12-1 and TT12-2 themselves superimpose with an rmsd value of 0.27 Å.

Influence of the Chiral Ligand on Oxaliplatin Binding to DNA. The platinum oxalato complex containing the (1*R*,2*R*)-diaminocyclohexane ligand (oxaliplatin) is pharmacologically more potent than the *S*,*S* enantiomer.[22−24] Solution studies of (2*R*,3*R*)-diaminobutaneplatinum(II), {(*R*,*R*)-(DAB)−Pt}$^{2+}$, complexes bound to duplex DNA suggest the presence of a hydrogen bond between the DAB nitrogen cis to the 3′-G of the GG lesion and the O6 of the 3′-guanine,[33] mediated only by the pseudoequatorial hydrogen atom of the NH_2 moiety. Such a feature has been observed previously in small molecule crystal structures of platinum(II) purine complexes containing achiral (di)amine ligands[37] and in a molecular modeling study of a platinated, single-stranded DNA.[38] The results described here provide structural proof for such a hydrogen-bonding interaction between a chiral ligand in a Pt(II) complex with the chiral DNA molecule to which it is coordinated (see Figure 6). Binding of the (*R*,*R*)-DACH or (*R*,*R*)-DAB ligand to platinum both locks the conformation of the C−N bond, thereby fixing the position of the hydrogen atoms of the NH_2 groups, and directs the pseudoequatorial hydrogen atom cis to the 3′-guanine to form a hydrogen bridge to the O6 of the nucleobase. Chaney et al.

(65) Gao, Y.-G.; Robinson, H.; van Boom, J. H.; Wang, A. H.-J. *Biophys. J.* **1995**, *69*, 559−568.
(66) Gao, Y.-G.; Sriram, M.; Wang, A. H.-J. *Nucleic Acids Res.* **1993**, *21*, 4093−4101.
(67) Larsen, K. P.; Toftlund, H. *Acta Chem. Scand.* **1977**, *A31*, 182−186.
(68) Bruck, M. A.; Bau, R.; Noji, M.; Inagaki, K.; Kidani, Y. *Inorg. Chim. Acta* **1984**, *92*, 279−284.
(69) Miller, M.; Harrison, R. W.; Wlodawer, A.; Appella, E.; Sussman, J. L. *Nature* **1988**, *334*, 85−86.
(70) Arnott, S.; Chandrasekaran, R.; Birdsall, D. L.; Leslie, A. G. W.; Ratliff, R. L. *Nature* **1980**, *283*, 743−745.
(71) Chandrasekaran, R.; Arnott, S. *J. Biomol. Struct. Dyn.* **1996**, *13*, 1015−1027.
(72) Kraulis, P. J. *J. Appl. Crystallogr.* **1991**, *24*, 946−950.
(73) Merritt, E. A.; Murphy, M. E. P. *Acta Crystallogr.* **1994**, *D50*, 869−873.

Table 3. Structures of 1,2-platinated DNA Models with a d(GpG) Unit

DNA model	bend ∠ (deg)				guanine dihedral angles	Pt displ from G plane (Å)
		Curves, MadBend	Freehelix, MadBend	3DNA, MadBend		
X-ray of d(pGpG)[5]	n/a	n/a	n/a	n/a	76−87	0.2, 5′ 0.4, 3′
X-ray of 12-mer[8]	∼39 and 55	28 and 26	24 and 26	27 and 28	28	1.3, 5′ 0.8, 3′
NMR of 12-mer[11]	∼78	80	52	80	49	0.8, 5′ 0.8, 3′
X-ray of 16-mer + HMG1 domA[14]	∼61	43	66	47	75	0.5, 5′ 0.2, 3′
DACH 12-mer[a]		30	24	29	25	1.3, 5′ 0.8, 3′

[a] This work.

correlated the higher cytotoxicity of oxaliplatin with the greater degree of translesion synthesis by mammalian polymerase β past oxaliplatin.[28] Such translesion synthesis induces mutations. The differences between the crystal structures of cisplatin and oxaliplatin bound to DNA reveal that only the latter has a hydrogen bond to the 3′ guanine. This result confirms the prediction by Chaney et al. that the oxaliplatin and cisplatin−GG adduct will show the greatest conformational differences in the vicinity of the 3′-G(Pt).

A remaining question is whether the observed differences in cytotoxicity for the various configurational isomers of oxaliplatin are modulated by differentiating reactions that occur prior to attack on DNA and/or whether such reactions occur when proteins interact with platinum lesions on DNA, forming ternary complexes.

Conclusion

An (*R*,*R*)-DACH platinum(II) 1,2-intrastrand d(GpG) cross-link in a DNA duplex with the same sequence as that previously investigated for cisplatin was synthesized, purified, and crystallized. Pt MAD data afforded the X-ray crystal structure of a non-cisplatin complex with a platinated DNA duplex. The overall geometry is relatively similar to that of the cisplatin-modified DNA, although the two adducts crystallize in two different space groups. A hydrogen bond forms between the pseudoequatorial NH of the (*R*,*R*)-DACH ligand and the O6 atom of the 3′-G of the d(GpG) lesion, affording experimental evidence for this kind of chiral interaction. The structure provides the first unambiguous evidence on a molecular level of how cisplatin and oxaliplatin differentially modify DNA. This finding suggests that the search for a better anticancer drug might be directed toward the design of molecules that form hydrogen bonds directly to DNA in the vicinity of the platinum lesion.

Acknowledgment. This work was supported by a grant from the National Cancer Institute. B.S. was supported by the Swiss National Science Foundation and the Novartis Foundation. We thank Prof. C. Drennan, Drs. Uta-Maria Ohndorf and Tzanko Doukov, and Mr. Mike Sintchak for helpful discussions and Prof. George Sheldrick for providing us with a modified version of his SHELXL97 program. We thank Dr. Frank J. Rotella for helping us to acquire the Pt MAD data at Argonne. Use of the Argonne National Laboratory Structural Biology Center beamlines at the Advanced Photon Source was supported by the U.S. Department of Energy, Office of Biological and Environmental Research, under Contract No. W-31-109-ENG-38. X-ray data were also collected at the Stanford Synchrotron Radiation Laboratory (SSRL), which is funded by the Department of Energy (BES, BER) and the National Institutes of Health (NCRR, NIGMS).

Supporting Information Available: Spectroscopic and crystallographic information for **3b** and **6** (PDF). This material is available free of charge via the Internet at http://pubs.acs.org.

IC010790T